

# Molybdenum gratings as a high-temperature refractory platform for plasmonic heat generators in the infrared

Sara Nunez-Sanchez<sup>1,2</sup>, Hugo Dominguez Andrade<sup>3</sup>, Jan Harwood<sup>3</sup>, Ian Bickerton<sup>3</sup>, Neil A. Fox<sup>3</sup>, Martin J. Cryan<sup>1</sup> ✉

<sup>1</sup>Department of Electrical and Electronic Engineering, Faculty of Engineering, University of Bristol, Queen's Building, University Walk, Bristol BS8 1TR, UK

<sup>2</sup>Departamento de Química Física & CINBIO, Universidade de Vigo, Vigo, Spain

<sup>3</sup>School of Chemistry, CVD Diamond Group, University of Bristol, Bristol BS8 1TL, UK

✉ E-mail: m.cryan@bristol.ac.uk

Published in *Micro & Nano Letters*; Received on 23rd February 2018; Revised on 24th April 2018; Accepted on 1st June 2018

The aim of this work is to study the heating efficiency of refractory microstructures by excitation of surface plasmon polaritons in the far infrared that can be used for high-temperature applications. The work has designed metal grating couplers on molybdenum films to maximise the absorption of a 10.6  $\mu\text{m}$  CO<sub>2</sub> laser light source. Molybdenum has been chosen since it is an industrial refractory metal combined with the fact that its optical properties in the far infrared are similar to gold but with stable high-temperature performance. Linear gratings have been used as plasmonic couplers on large area substrates produced by laser milling. Real-time absolute temperature measurements have been performed showing a 42% increase in the maximum achievable temperature from 702 to 985 K.

**1. Introduction:** Heat-assisted chemistry and material science always require advances in substrate platforms that allow stable operation at high temperatures. This is particularly important in experimental techniques where high temperatures are mandatory for testing of thermionic and thermoelectric materials [1] and promoting chemical reactions [2], and for heat-assisted deposition of materials [3] such as epitaxial growth by pulsed laser deposition [4] or electrodeposition [5]. Platforms based on resistive heating have been extensively used [6, 7], however, light-assisted high-temperature platforms without possible spurious electrical currents are essential in, for example, the characterisation of thermal electron emission from thermionic materials [8].

Plasmonics is an already well-known photonic tool which allows us to transform absorbed light into heat by concentrating high electric fields in subwavelength dimensions (nano and micro volumes) [9]. The boundary condition to support surface plasmon polaritons within a metal–dielectric interface is related to the relative values of the real part of the permittivity between the two media. Thus, the metal should achieve values of the real part of the permittivity ( $\epsilon$ ) negative enough to fulfil the mode condition ( $\text{Real}\{\epsilon_{\text{metal}}\} < -\text{Real}\{\epsilon_{\text{dielectric}}\}$ ). Due to this requirement, plasmonic research in the visible range has been focused mainly in structures formed by noble metal nanostructures with more compatible optical properties in the visible range [10]. Noble metals allow high confinement of the field at the metal–dielectric interface and show low loss in the visible range (low values of the imaginary part of the permittivity). However, they are not practical for high-temperature applications due to their low bulk melting and softening points [11]. In contrast, refractory metals have excellent thermal stability at high temperatures with melting points above 2000°C. Moreover, they are chemically inert and stable against creep deformation at high temperatures combined with good electrical and heat conductivity [12]. However, traditional refractory metals such as molybdenum or tungsten cannot support surface plasmon polaritons in the visible range due to their positive values of the real part of the permittivity. Recent works show that refractory alloys such as titanium nitride could mimic the optical properties of noble metals in the visible range with large bulk melting points [13, 14]. However, these metallic alloys are not chemically stable, for example, when working in an oxygen atmosphere

[15–17]. Therefore, they cannot be long-term stable refractory platforms in reactive environments or in ambient conditions such as air [18]. The aim of our work is to show the potential of a traditional refractory metal such as molybdenum as a refractory plasmonic platform for high-temperature applications assisted by light but, focusing the problem in a different wavelength window, in the infrared range instead in the visible range.

**2. Results:** The optical properties of molybdenum have been determined a number of years ago during the 80s. The plasma wavelength of molybdenum was estimated as 130 nm by Ordal *et al.* [19]. In the wavelength range between 130 and 800 nm, the real part of the permittivity of molybdenum oscillates between positive and negative values, showing a hybrid nature between a metal and a lossy dielectric. However, for wavelengths larger than the crossover wavelength (around 850 nm), the real part of the permittivity of molybdenum is similar to gold in the infrared range [13]. Fig. 1b shows the values of the real part of the permittivity in the infrared range for molybdenum and gold. Both metals fulfil the conditions to support surface plasmon polaritons at an air–metal interface, obtaining a similar surface polariton dispersion curve (see Fig. 1a).

As we are located far from the plasma frequency, the real values of the permittivity achieved are strongly negative, meaning that the surface plasmon polariton dispersion curve is located close to the edge of the light cone.

Experimental thermoplasmonics at high temperatures is an under-explored area, partially due to the poor thermal stability of traditional plasmonic materials as Ag or Au combined with the difficulty of obtaining in-situ temperature measurements in real samples. For our experiment, we have developed an experimental set-up to do real-time direct temperature measurements on large area samples [8]. Temperature measurements have been performed under vacuum conditions ( $P=1 \cdot 10^{-6}$  Torr) in order to avoid thermal losses due to air convection. Also, the sample holder was made of quartz which has a very low thermal conductivity in order to minimise the heat loss *via* heat conduction from sample to holder. Our light source was a linear polarised CO<sub>2</sub> laser at 10.6  $\mu\text{m}$ , guided to the sample by gold mirrors. The laser spot is around 5 mm in diameter with a Gaussian intensity profile on

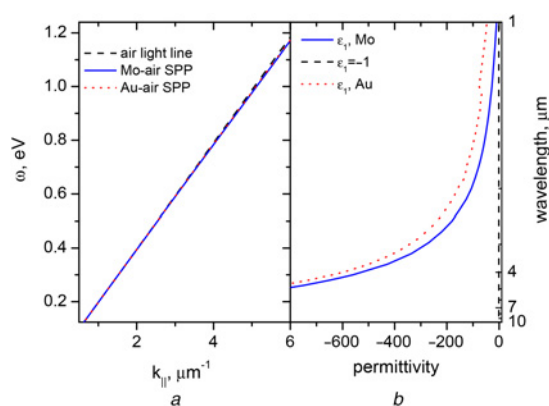


**Fig. 1** Optical characteristics of gold and molybdenum  
*a* Analytic dispersion curve of surface plasmon polaritons supported by an air-molybdenum interface (blue line) and an air-gold interface (red dotted line). Dashed black line represents the light line [20]  
*b* Values of the real part of the permittivity of molybdenum (blue continuous line) and gold (red dotted line) in the wavelength range from 1 to 12  $\mu\text{m}$ . The black dashed line indicates the optical properties required to fulfil the surface polariton mode condition. Optical properties obtained from [19, 21]

the surface of the sample. The laser is set at normal incidence on the patterned side of the sample. The temperature probes used were a type-K thermocouple pressed against the non-patterned side of the sample and a two colour infrared pyrometer (Land Instruments Ltd). In order to avoid any interaction between the laser beam and the temperature probes, all the temperature measurements have been performed on the back side of the sample, opposite to the grating. The thermocouple has been used to measure the temperatures below 973 K while the two-colour pyrometer detector was used for higher temperatures. Laser heating is a fast process, so in order to allow the system to achieve a stable temperature, all temperature measurements have been recorded after a few minutes to allow the system to reach steady-state conditions. The experimental system is described in detail elsewhere [8].

Since we are using a laser light source, the simplest device to excite a surface plasmon polariton is a linear metal grating. The metal grating allows the light to access wave vector values below the light cone by diffraction, thus exciting surface plasmon polaritons modes. Fig. 2*a* shows the analytical dispersion curve

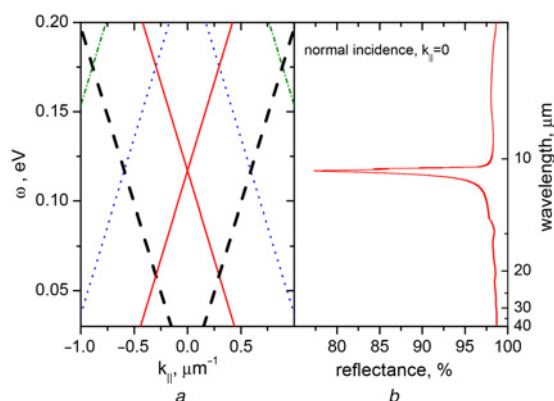


**Fig. 2** Optical characteristics of a molybdenum grating  
*a* Analytical dispersion curve of surface plasmon polaritons propagating in a molybdenum grating of period 10.5  $\mu\text{m}$ . Black line dashed lines correspond to the light cone lines. Red continuous, blue dotted and green dotted-dashed curves indicated the zero-, first- and second-order light of the molybdenum grating  
*b* Reflectance associated to the same grating at normal incidence ( $k_{||}=0$ , see Fig. 2*a*) showing a minimum at reflectance at 10.6  $\mu\text{m}$  when the surface plasmon polariton mode is excited

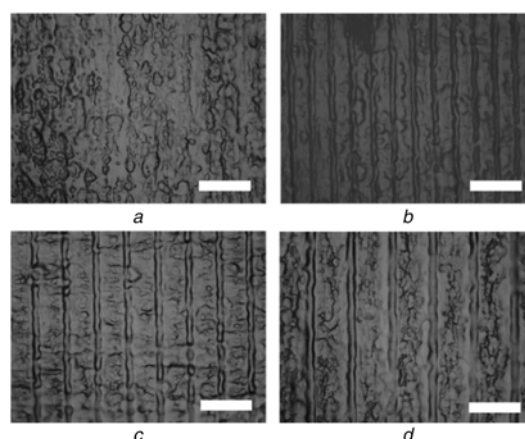
for a molybdenum grating of period 10.5  $\mu\text{m}$  in air environment. Due to our illumination conditions we need to excite the surface plasmon at normal incidence (parallel component of wavevector,  $k_{||}=0$ ), therefore we have designed molybdenum gratings with a period similar to the incident wavelength. The fine tuning of the period has been determined by finite difference time domain modelling (Lumerical Solutions) of the optical response of a molybdenum grating with similar parameters to that obtained experimentally (Fig. 2*b*).

The refractory plasmonic couplers have been produced on commercial industrial molybdenum foil (thickness of 0.25  $\mu\text{m}$ , purity of 99.9% and anneal tempered; supplied by Goodfellow Cambridge Ltd). In order to be able to perform direct temperature measurements, the homogeneous gratings have been produced in large area samples of 1  $\text{cm}^2$ . The structures have been patterned by laser milling using a Nd:YAG laser ( $\lambda=532$  nm,  $t=10$ –15 ns (nominal), 15 kHz repetition rate, Alpha III system, Oxford Lasers). The Gaussian spatial energy distribution of the laser beam profile combined with the high ablation threshold of molybdenum allowed us to obtain features smaller than the laser spot size at the focus position.

In order to obtain the same groove morphology in all samples, they have all been produced at 4.8  $\text{J cm}^{-2}$  with the same repetition rate (15 kHz) and a laser firing distance of 1  $\mu\text{m}$ . Using a 10  $\mu\text{m}$  diameter laser spot with a 40 mm focal lens, we obtain 3  $\mu\text{m}$  diameter circular marks on the molybdenum substrate. Flat substrates are required in order to be at the same focus position in all the areas of the raw substrate to obtain uniformly patterned samples. Therefore, in order to avoid any bending of the molybdenum substrates at the edges by a mechanical cutting process, the substrates have been prepared by laser cutting using the Nd:YAG laser system at 74.4  $\text{J cm}^{-2}$ , 1 kHz repetition rate and with a laser firing distance of 0.2  $\mu\text{m}$ . A bare molybdenum substrate of the same size and molybdenum batch without a plasmonic coupler has been used as a reference sample.

Molybdenum linear gratings with different periods have been produced in order to check the effects of the plasmon coupling conditions. Fig. 3 shows optical microscope images of the surface of three different grating couplers with a 10.5  $\mu\text{m}$  pitch (10P), 15.0  $\mu\text{m}$  pitch (15P) and 20.0  $\mu\text{m}$  pitch (20P).

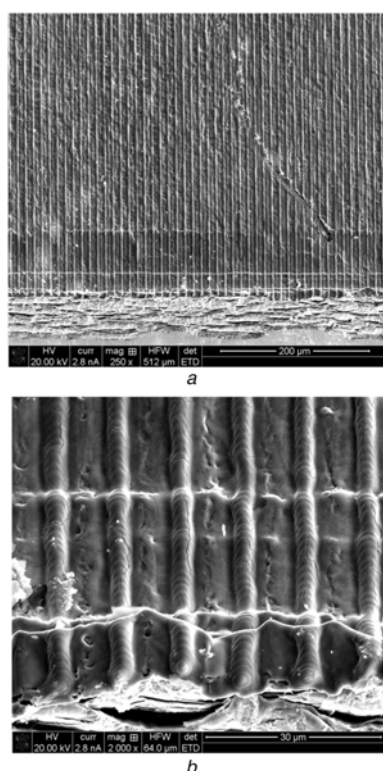
The industrial molybdenum surface of the molybdenum foil is not flat (see Fig. 3*a*). All the gratings show the same groove geometry with slight local differences due to the surface roughness



**Fig. 3** Optical microscope images of the surface of thermally tested molybdenum samples  
*a* Bare sample and laser-structured samples with periods of  
*b* 10.5  $\mu\text{m}$  (10P)  
*c* 15.0  $\mu\text{m}$  (15P)  
*d* 20.0  $\mu\text{m}$  (20P)  
 Objective magnification 50 $\times$ . Scale bar 25  $\mu\text{m}$

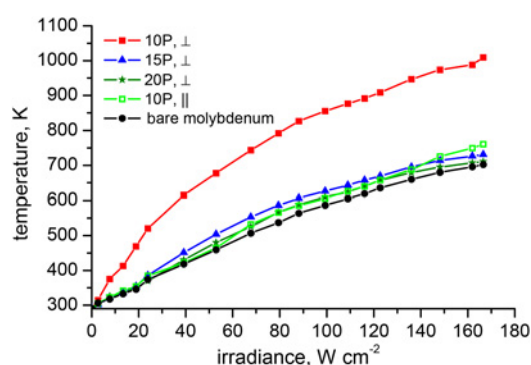
of the bare molybdenum substrates (see Fig. 3a). The morphology of the samples will be the convolution of the engraved pattern and the intrinsic surface morphology of the molybdenum substrate. The substrate roughness is going to add some randomness to our samples but we considered that the response will show an average effect which is similar between samples. Analysing the optical images combined with surface electron microscopy images (Fig. 4) we can infer that the width of the grating grooves is around  $3.3\ \mu\text{m}$ . The depth of the groove changes as a function of the roughness and has an average value of  $0.5\ \mu\text{m}$ .

Fig. 5 shows the temperature achieved in the four samples at different values of laser irradiance. All samples were obtained



**Fig. 4** SEM images of the edge of the laser-structured molybdenum grating with a period of  $10.5\ \mu\text{m}$  (10P)

a  $250\times$  magnification  
b  $2000\times$  magnification



**Fig. 5** Temperature versus laser power irradiance plots of a bare molybdenum substrate (black circular dots) and three molybdenum gratings with the laser polarisation perpendicular to the grating grooves. 15P corresponds to the grating with the period  $15\ \mu\text{m}$  (blue triangular dots). 20P corresponds to the grating with period  $20\ \mu\text{m}$  (green start dots). 10P corresponds to the grating with a period of  $10.5\ \mu\text{m}$  (red full square dots). Also we have included the temperature achieved at different laser power intensities with the polarisation of the laser parallel to the gratings grooves for 10P sample (green empty square dots)

from the same molybdenum foil. Therefore, all the grating results are compared with the bare molybdenum in order to eliminate the effects originated from the roughness of the molybdenum foil.

The bare molybdenum substrate achieves  $702\ \text{K}$  at maximum laser power ( $166\ \text{W cm}^{-2}$ ). In order to couple to the surface plasmon, the laser linear polarisation is perpendicular to the linear grating grooves. The coupling condition will only be fulfilled at normal incidence for the molybdenum grating with a  $10.5\ \mu\text{m}$  period (10P). When the coupling condition is matched we observe an increase in the temperature in comparison with the bare molybdenum substrate for all the laser powers, achieving a maximum temperature of  $985\ \text{K}$ . This corresponds to an increase of 42% in temperature for large pumping powers. In comparison, the temperature achieved for molybdenum gratings 15P and 20P under the same illumination conditions is practically the same as for the bare molybdenum substrate. For linear gratings with a period of 15 and  $20\ \mu\text{m}$  we are not able to couple to the surface plasmon at normal incidence conditions, and it behaves as a flat substrate. In order to corroborate the surface plasmon excitation phenomenon, we have performed the same measurements but with the polarisation of the  $\text{CO}_2$  laser parallel to the grating grooves. Under this illumination condition, we cannot couple to the surface plasmon and the temperature achieved is similar to the bare molybdenum substrate, showing no surface plasmon polariton coupling effects.

**3. Conclusions:** This work demonstrates that plain molybdenum in industrial foil format could be a good candidate for refractory high-temperature platforms with broad applications in material science, chemistry and photonics. We also note that molybdenum has optical properties that allows coupling to surface plasmons in the telecommunication wavelength from  $1.3$  to  $1.7\ \mu\text{m}$ . Therefore, molybdenum could be a useful material for optically activated thermal switches for integrated photonics applications. Also the ability to produce photonic structures compatible with traditional industrial bulk materials such as molybdenum foil could inspire new ideas for implementation of light-induced local heaters in industrial devices. It still remains open to study how to further improve the temperature achieved in these molybdenum plasmonic couplers by optimising, groove morphology and in-plane periodic geometries. In future work, we intend to analyse in detail the complete system using finite-element analysis tools such as COMSOL.

**4. Acknowledgment:** The authors acknowledge the Engineering and Physical Sciences Research Council Grant, grant no. EP/K030302/1 for funding. Data shown in this paper is accessible via the University of Bristol data repository: doi: 10.5523/bris.762r475j6kpy2u1o2lthpq0s2.

## 5 References

- [1] Suzuki M., Ono T., Sakuma N., *ET AL.*: 'Low-temperature thermionic emission from nitrogen-doped nanocrystalline diamond films on n-type Si grown by MPCVD', *Diam. Relat. Mater.*, 2009, **18**, pp. 1274–1277
- [2] Baffou G., Quidant R.: 'Nanoplasmonics for chemistry', *Chem. Soc. Rev.*, 2014, **43**, pp. 3898–3907
- [3] Wahl G., Stadel O., Gorbenko O., *ET AL.*: 'High-temperature chemical vapor deposition. An effective tool for the production of coatings', *Pure Appl. Chem.*, 2000, **72**, pp. 2167–2175
- [4] Hegde M.: 'Epitaxial oxide thin films by pulsed laser deposition: retrospect and prospect', *J. Chem. Sci.*, 2001, **113**, pp. 445–458
- [5] Mkawi E.M., Ibrahim K., Ali M.K.M., *ET AL.*: 'Influence of substrate temperature on the properties of electrodeposited kesterite  $\text{Cu}_2\text{ZnSnS}_4$  (CZTS) thin films for photovoltaic applications', *J. Mater. Sci. Mater. Electron.*, 2014, **26**, pp. 222–228
- [6] Falconer J.L., Schwarz J.A.: 'Temperature-programmed desorption and reaction: applications to supported catalysts', *Catal. Rev.*, 1983, **25**, pp. 141–227

- [7] Engelhart D.P., Grätz F., Wagner R.J.V., *ET AL.*: 'A new Stark decelerator based surface scattering instrument for studying energy transfer at the gas-surface interface', *Rev. Sci. Instrum.*, 2015, **86**, p. 043306
- [8] Andrade H.D.: 'Work function modification studies for energy applications: Surface chemical functionalisation to plasmonic tuning', PhD Thesis, Bristol, 2015
- [9] Baffou G., Quidant R.: 'Thermo-plasmonics: using metallic nanostructures as nano-sources of heat', *Laser Photonics Rev.*, 2013, **7**, pp. 171–187
- [10] West P.R., Ishii S., Naik G.V., *ET AL.*: 'Searching for better plasmonic materials', *Laser Photonics Rev.*, 2010, **4**, pp. 795–808
- [11] Boltasseva B.A., Shalaev V.M.: 'All that glitters need not be gold', *Science*, 2015, **347**, pp. 1308–1310
- [12] Tietz T., Wilson J.: 'Behavior and properties of refractory metals' (University of Tokio Press, Tokio, Japan, 1965)
- [13] Guler U., Boltasseva A., Shalaev V.M.: 'Refractory plasmonics', *Science*, 2014, **344**, pp. 263–264
- [14] Li W., Guler U., Kinsey N., *ET AL.*: 'Refractory plasmonics with titanium nitride: broadband metamaterial absorber', *Adv. Mater.*, 2014, **26**, pp. 7959–7965
- [15] Saha N.C., Tompkins H.G.: 'Titanium nitride oxidation chemistry: an x-ray photoelectron spectroscopy study', *J. Appl. Phys.*, 1992, **72**, p. 3072
- [16] Suni I., Sigurd D., Ho K.T., *ET AL.*: 'Thermal oxidation of reactively sputtered titanium nitride and hafnium nitride films', *J. Electrochem. Soc.*, 1983, **130**, pp. 1210–1214
- [17] Bagheri S., Zgrabik C.M., Gissibl T., *ET AL.*: 'Large-area fabrication of TiN nanoantenna arrays for refractory plasmonics in the midinfrared by femtosecond direct laser writing and interference lithography', *Opt. Mater. Express*, 2015, **5**, pp. 2625–2633
- [18] Yin Y., Hang L., Zhang S., *ET AL.*: 'Thermal oxidation properties of titanium nitride and titanium–aluminum nitride materials — a perspective for high temperature air-stable solar selective absorber applications', *Thin Solid Films*, 2007, **515**, pp. 2829–2832
- [19] Ordal M.A., Bell R.J., Alexander R.W., *ET AL.*: 'Optical properties of Al, Fe, Ti, Ta, W, and Mo at submillimeter wavelengths', *Appl. Opt.*, 1988, **27**, pp. 1203–1209
- [20] Barnes W.L., Dereux A., Ebbesen T.W.: 'Surface plasmon subwavelength optics', *Nature*, 2003, **424**, pp. 824–830
- [21] Palik E.D.: 'Handbook of optical constants of solids' (Academic Press, San Diego, CA, 1998)